Characteristics of Flare Acceleration Regions using Combined X-ray and Radio Observations

Hamish Reid[1] Nicole Vilmer[1]
Eduard Kontar[2]

[1]Observatoire de Paris [2]University of Glasgow

Motivation

Using remote observations, can we discern some properties of flare acceleration regions?

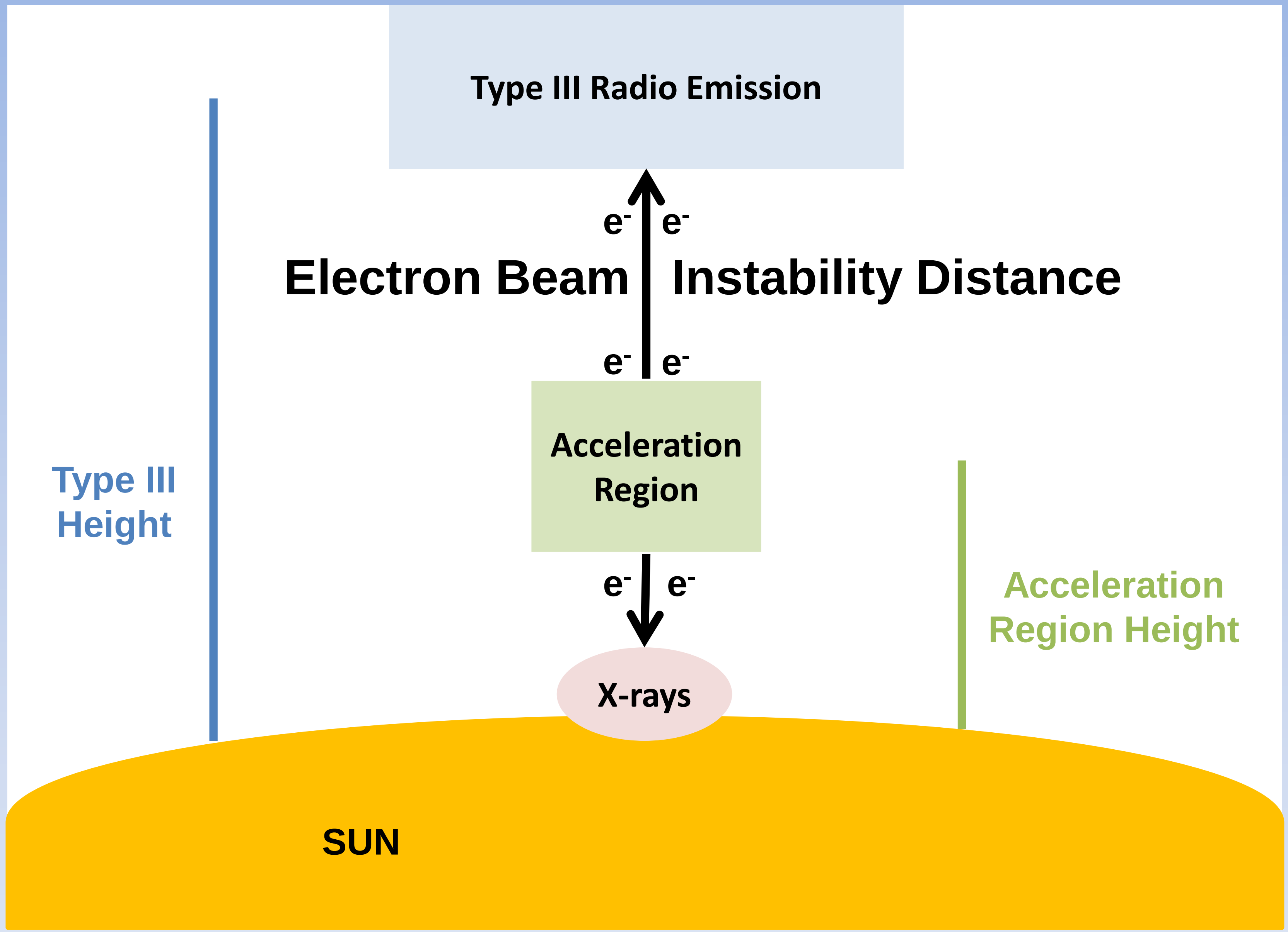
Type III Radio Emission
e- e-
Electron Beam Instability Distance
e- e-
Acceleration Region
e- e-
X-rays
Type III Height
Acceleration Region Height
SUN

Analytical Relation

Initial Electron Beam

$$f_0(v, r, t=0) \propto v^{-\alpha} \exp\left(\frac{-|r|}{d}\right)$$

Beam generates Langmuir waves when its growth rate is larger than the background plasma collisional absorption.

$$\frac{\partial f}{\partial v}$$

At instability distance
Δr = h$_{typeIII}$ – h$_{acceleration.}$

$$\Delta r = d\left(\alpha + \frac{v_c n}{\pi \omega_{pe}} v g_0(v)^{-1}\right)$$

Very Small

$$h_{typeIII} = d\alpha + h_{acceleration}$$

Finding Suitable Events

RHESSI flare list **http://hesperia.gsfc.nasa.gov/hessidata/dbase/hessi_flare_list.txt**
PHOENIX II burst list **http://soleil.i4ds.ch/solarradio/data/BurstLists/1998-2010_Benz/**

- Event had to occur between 08:00 and 16:00 UT for the PHOENIX II Spectrograph.
- Events had to be observed by RHESSI – not in night time or the SAA.
- Type III radio burst had to be between 4000 – 100 MHz for PHOENIX II.

14,174 flares and 1,046 type III bursts

- Events had to have a type III radio burst and an X-ray Flare at the same time..
- The peak of the X-ray emission had to occur at the same time as the type III burst.

205 correlated events

Finding Suitable Events

▪X-ray emission had to be impulsive – peak flux / duration > 0.1

159 events

We checked manually:

▪X-ray emission had to be strong enough to obtain a reasonable X-ray spectrum.

▪Type III radio burst had to occur long enough for a reasonable number of points.

▪Had to be an absence of decimetric emission to obtain the type III starting frequency.

31 possible candidates

Type III Example at High Frequency

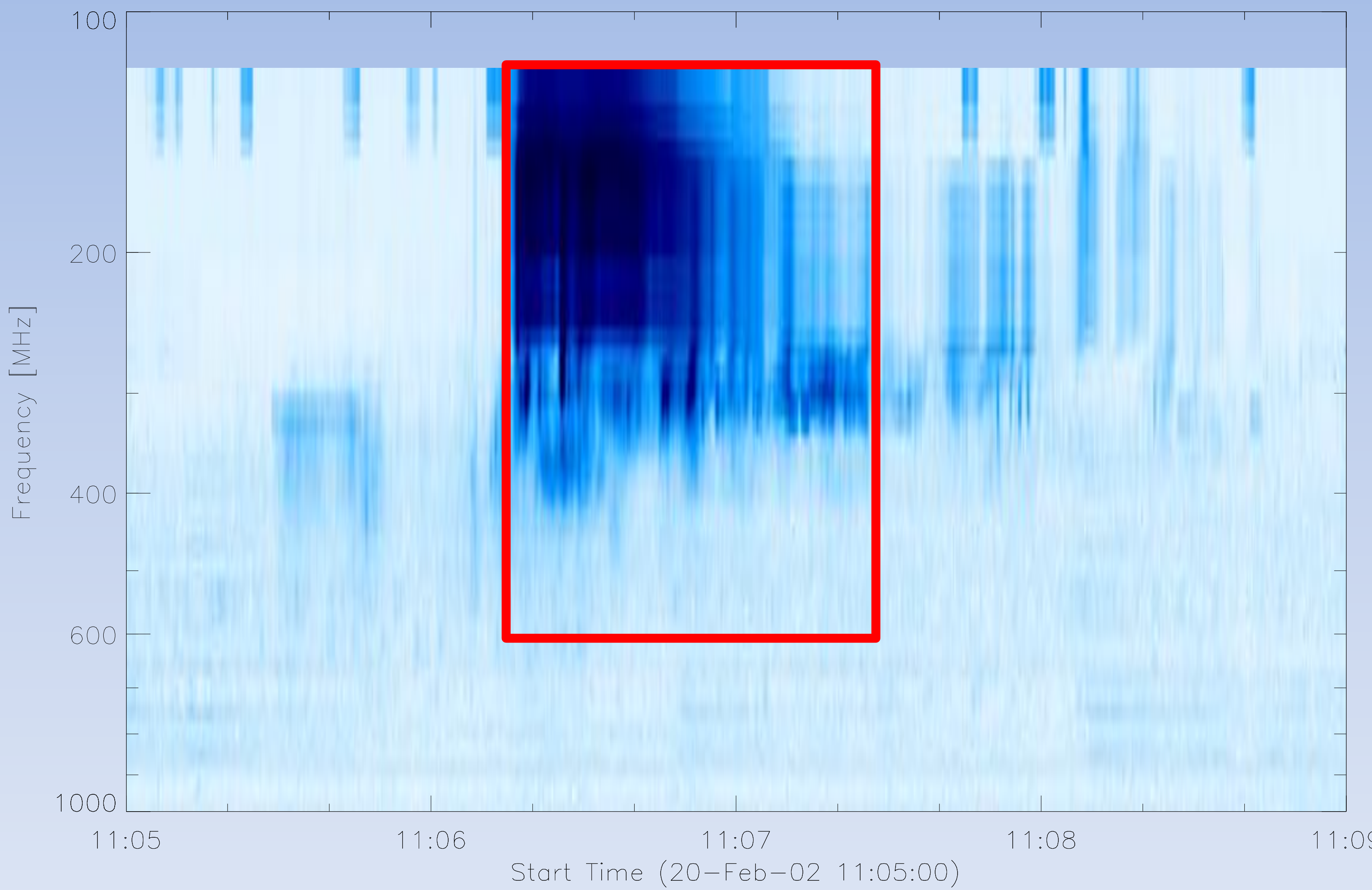

Correlated Events

Background is the radio dynamic spectrum for the type III burst for the five best correlated events. The resolution has been reduced to 2 s to fit with RHESSI.

Green stars are the starting frequency – the highest frequency of the type III burst above a certain threshold

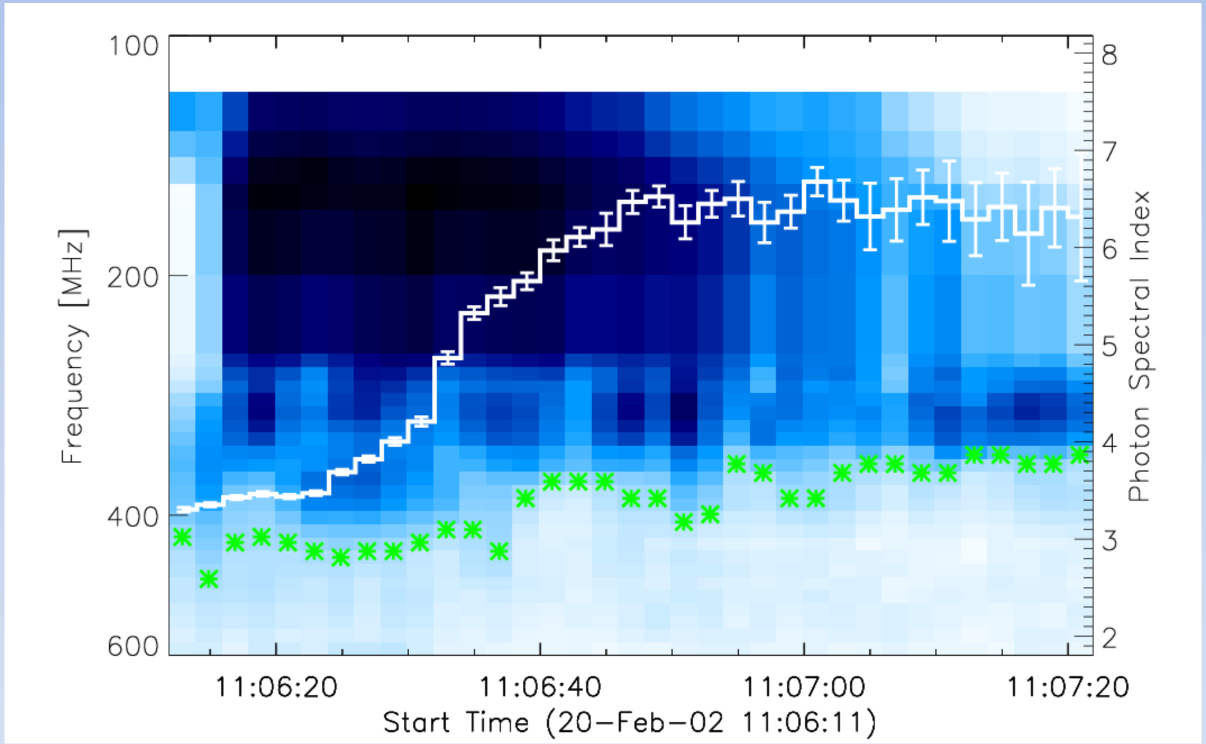

White line is the spectral index of the X-ray photons found from a thermal and power-law fit to the data.

15 events with a good correlation (coefficient above 0.65)

Starting Frequency vs Photon Spectral Index

We obtained errors on the spectral index from the power-law fit to the data.
We assumed one frequency channel as the error on the starting frequency.

A linear correlation can be observed between the photon spectral index and the starting frequency of the type III radio burst.

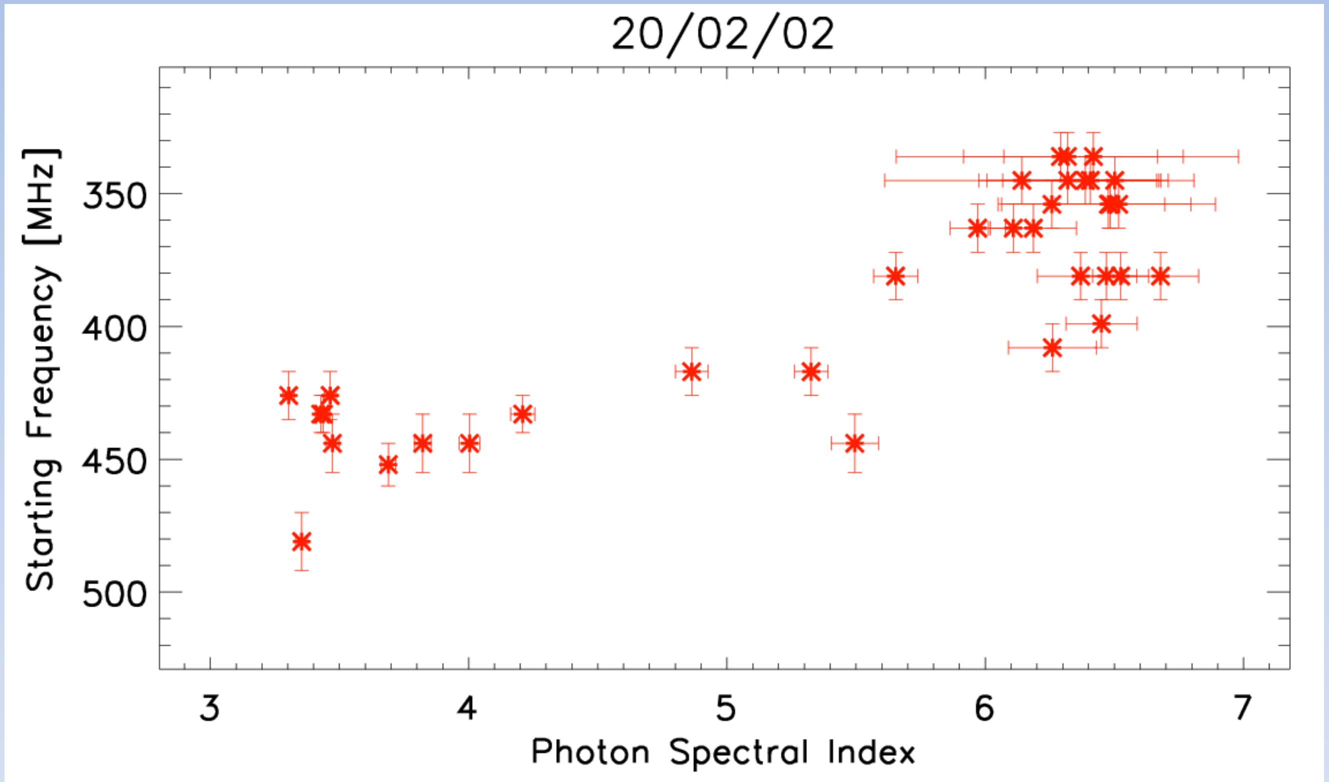

Estimating Acceleration Region Parameters

Starting Frequency ------> **Starting Height** with a density model.
Photon Spectra ------> **Electron Spectral Index** with the thick target model.

We use the intercept and gradient from a linear fit to the data to obtain an estimate on $h_{acceleration}$ and d respectively.

Top and bottom green lines are the extremes of the fit to the data

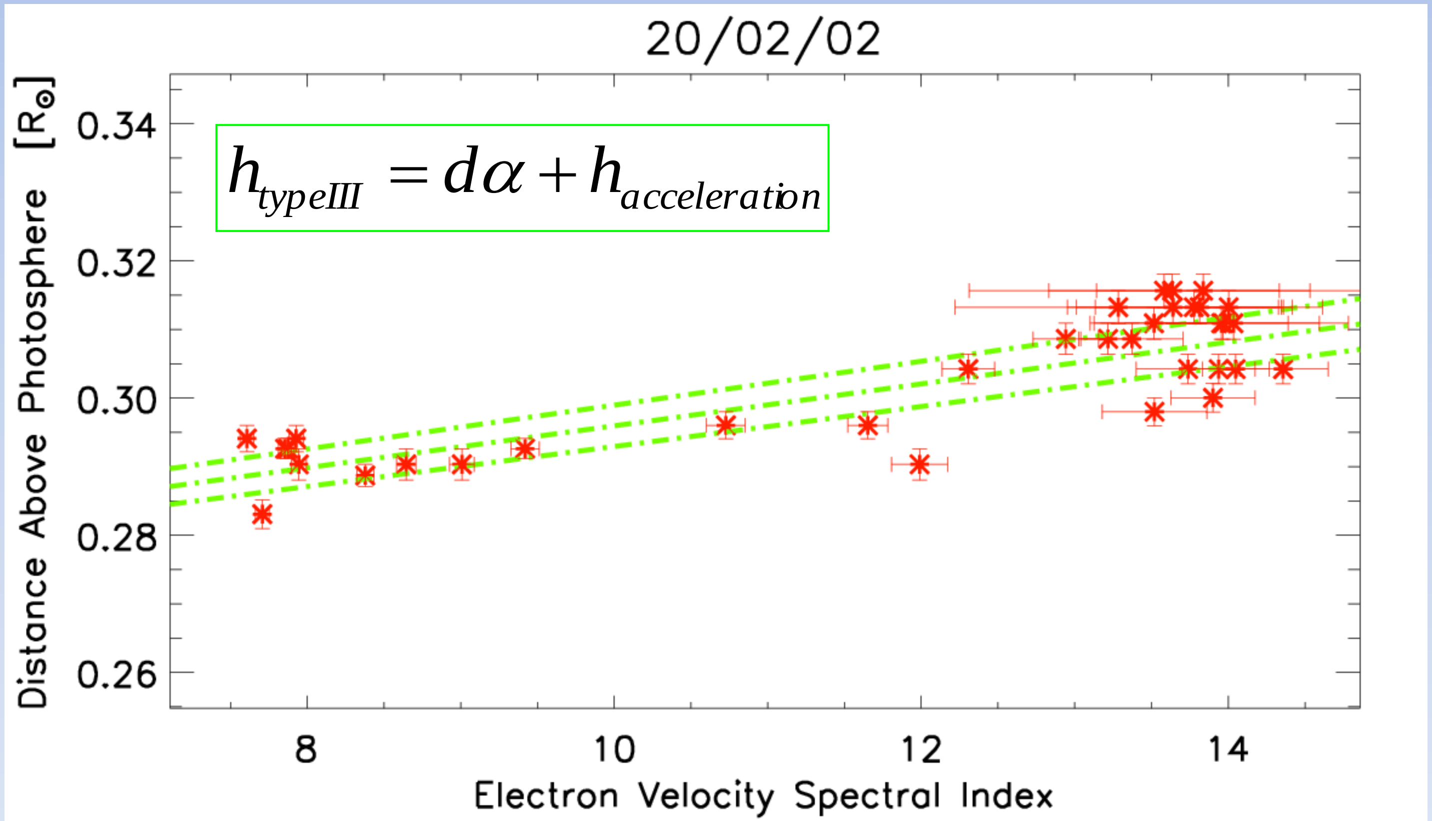

11 events with a sensible prediction

Flare Morphology

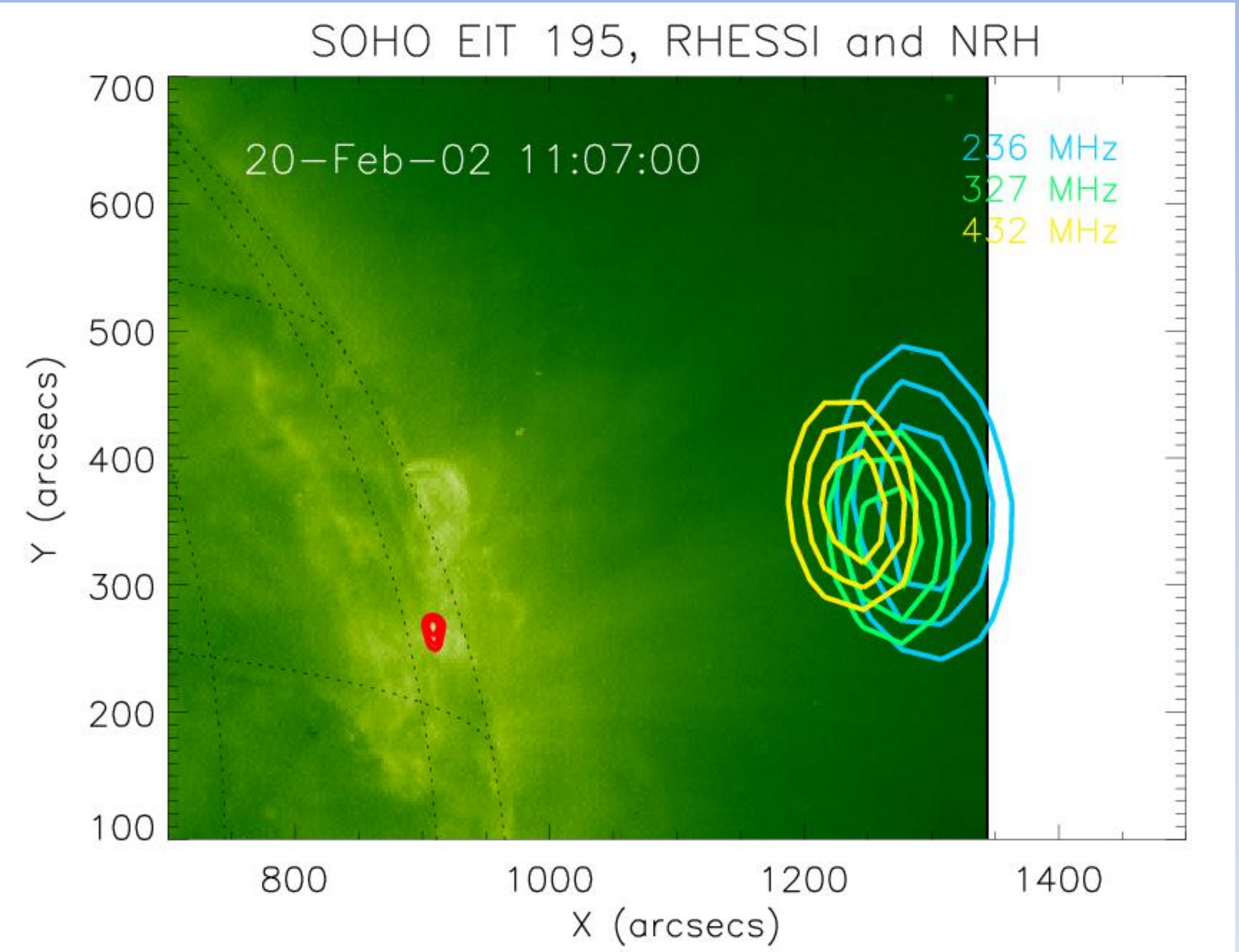

9 events with radio heliograph data

Flare Morphology

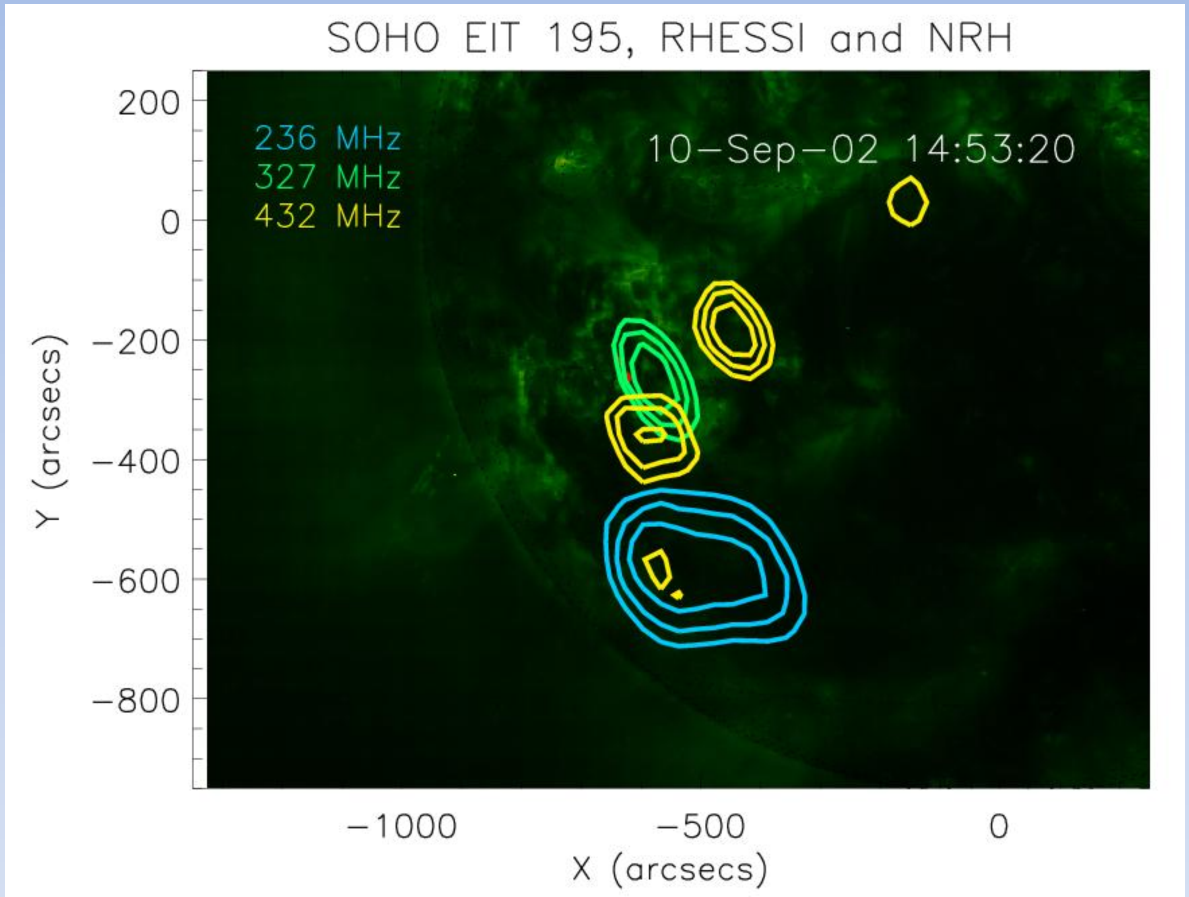

Not all of the events showed the simple morphology for the radio emission

6 events with satisfy all criteria

Parameters for the acceleration regions

Date	Correlation Coefficient	h_{acc}	h_{acc} Error	d	d Error
20/02/2002	0.84	180 Mm	1.1 Mm	2.1 Mm	0.1 Mm
19/07/2002	0.78	113 Mm	12 Mm	7.7 Mm	1.2 Mm
10/03/2003	0.89	76 Mm	9.6 Mm	10.8 Mm	1.0 Mm
18/03/2003	0.70	46 Mm	5.8 Mm	11.7 Mm	0.6 Mm
12/06/2003	0.69	78 Mm	3.9 Mm	7.5 Mm	0.3 Mm
25/07/2004	0.86	99 Mm	6.3 Mm	8.4 Mm	0.6 Mm

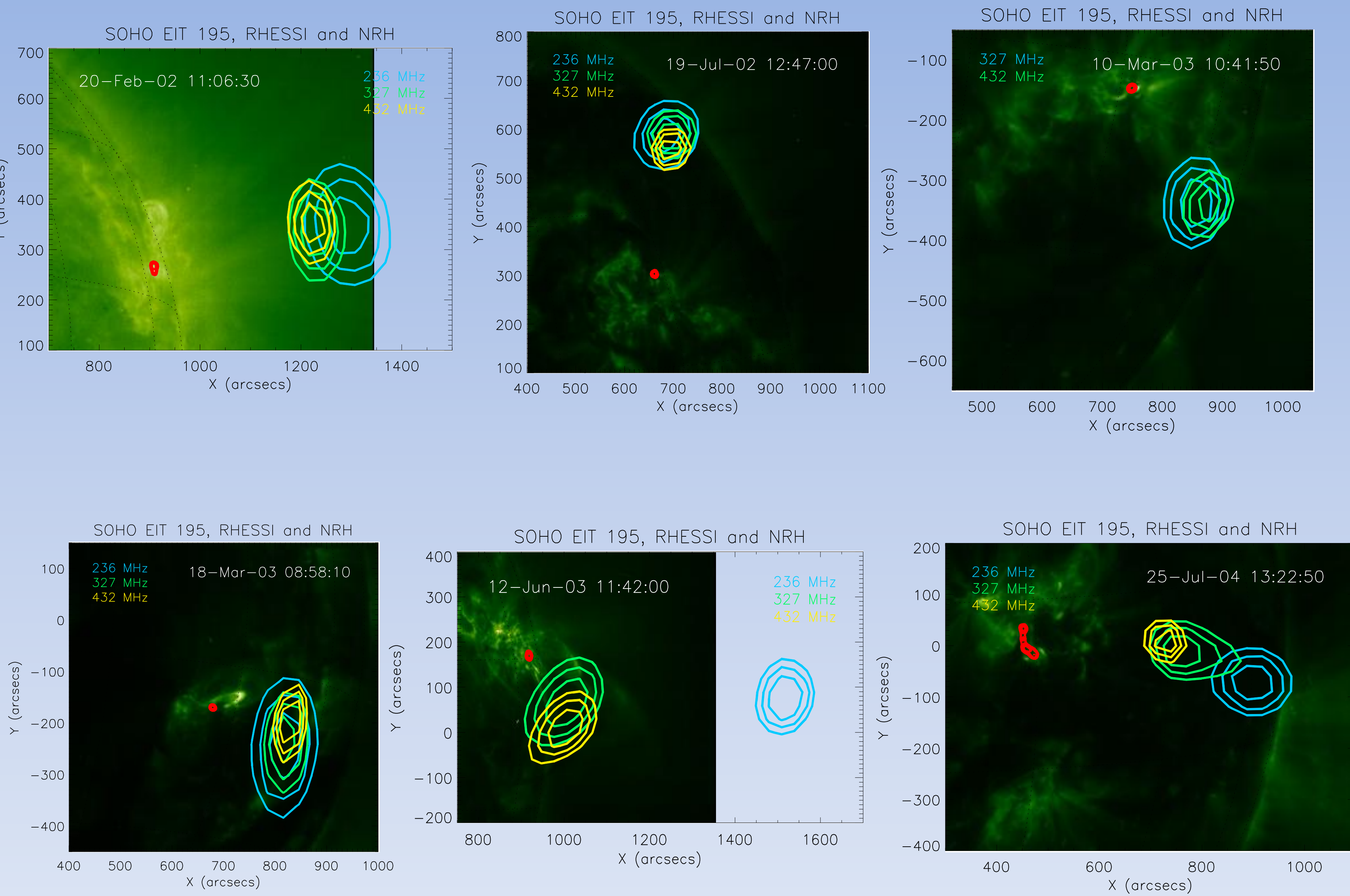
SOHO EIT 195, RHESSI and NRH
20-Feb-02 11:06:30
236 MHz
327 MHz
432 MHz
X (arcsecs)
SOHO EIT 195, RHESSI and NRH
19-Jul-02 12:47:00
236 MHz
327 MHz
432 MHz
Y (arcsecs)
X (arcsecs)
SOHO EIT 195, RHESSI and NRH
10-Mar-03 10:41:50
327 MHz
432 MHz
Y (arcsecs)
X (arcsecs)
SOHO EIT 195, RHESSI and NRH
18-Mar-03 08:58:10
236 MHz
327 MHz
432 MHz
Y (arcsecs)
X (arcsecs)
SOHO EIT 195, RHESSI and NRH
12-Jun-03 11:42:00
236 MHz
327 MHz
432 MHz
Y (arcsecs)
X (arcsecs)
SOHO EIT 195, RHESSI and NRH
25-Jul-04 13:22:50
236 MHz
327 MHz
432 MHz
Y (arcsecs)
X (arcsecs)

Discussion

- Acceleration region is quite high in the corona with respect to some previously reported analysis (e.g. time-of-flight). – Extra physics?

- Size of the acceleration region is large enough for a high number of particles to be accelerated – what would be the consequences if it was smaller?

- The simple scenario is not very common in solar flares....

- How do the assumptions hold up to reality?

Effect of the Density Model

Using an exponential density model of the form where the normalisation is found from Paesold et al (2001)

$$n(r) = A\exp(r / r_n)$$

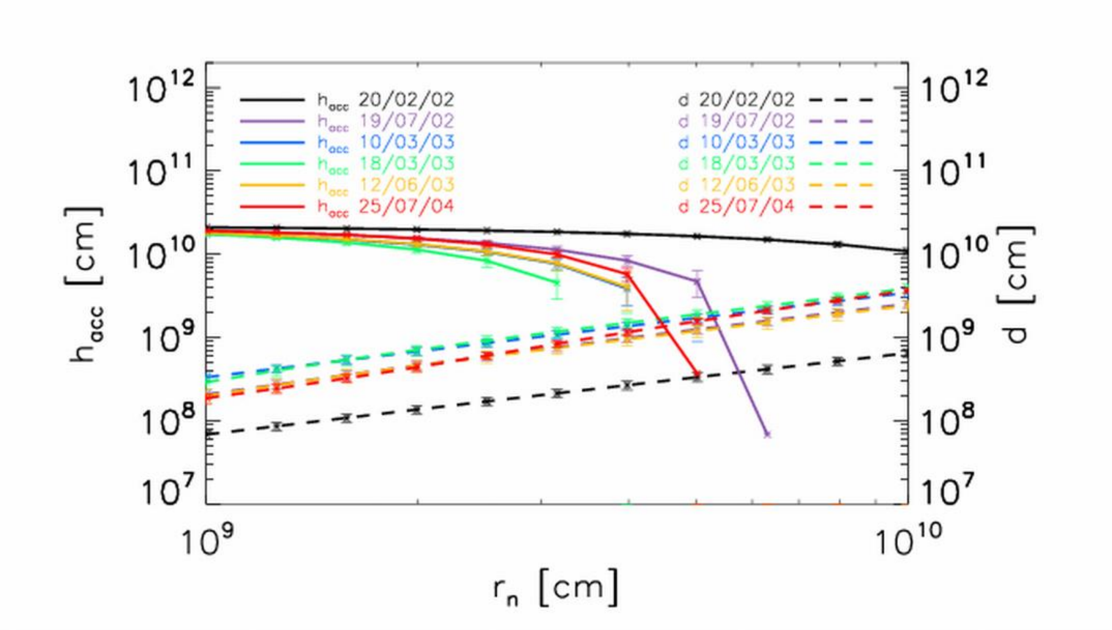

Changing the density gradient affects the size linearly but the realistic density gradients cover a small range in log space.

Changing the density gradient affects the height in a minimal way.

Changing the scale height (A) raises or lowers the height but does nothing to the size.

Conclusions

- We have used X-ray and radio observations to predict the height and size of some flare acceleration regions.
- We found acceleration sizes around 10^9 cm
- We found heights around 10^{10} cm, situated in the high corona.
- Only some events showed a simple morphology applicable for the study.
- Changing the coronal density model weakly affects the deduced parameters.

Extra Slides

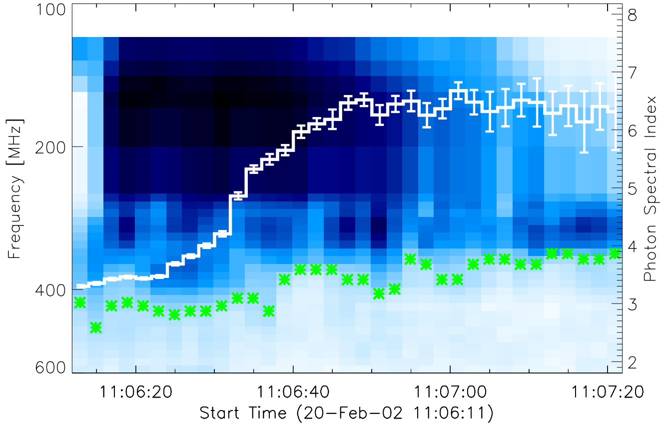
Frequency [MHz]
Photon Spectral Index
Start Time (20–Feb–02 11:06:11)

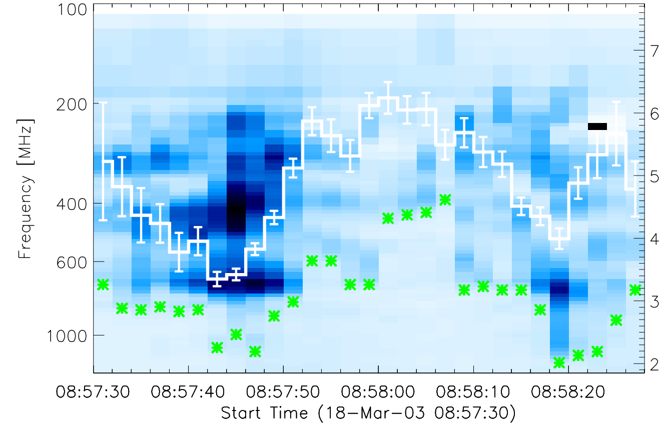
Frequency [MHz]
Photon Spectral Index
Start Time (18–Mar–03 08:57:30)

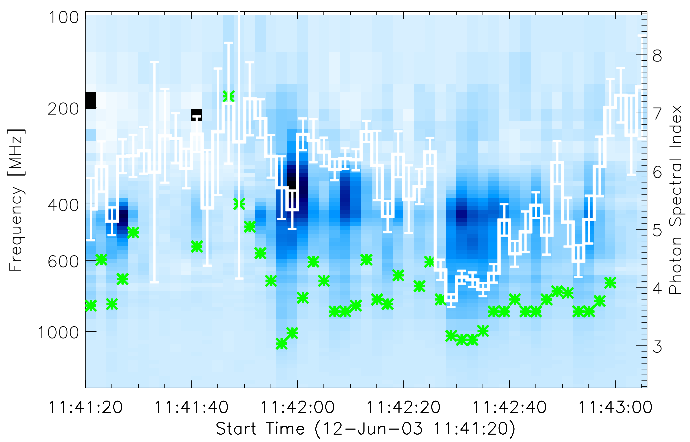
Frequency [MHz]
Photon Spectral Index
Start Time (12–Jun–03 11:41:20)

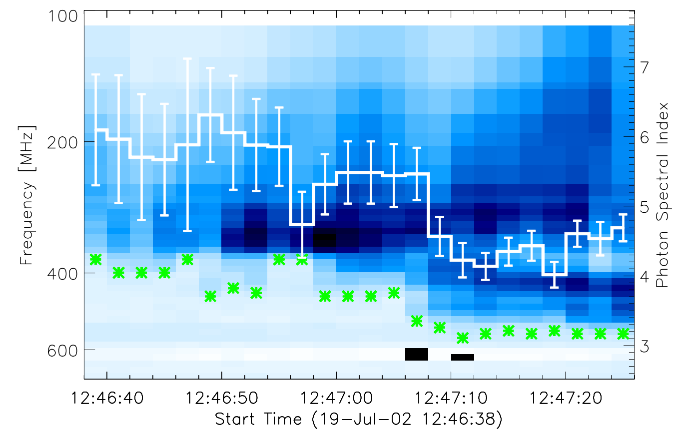
Frequency [MHz]
Photon Spectral Index
Start Time (19–Jul–02 12:46:38)

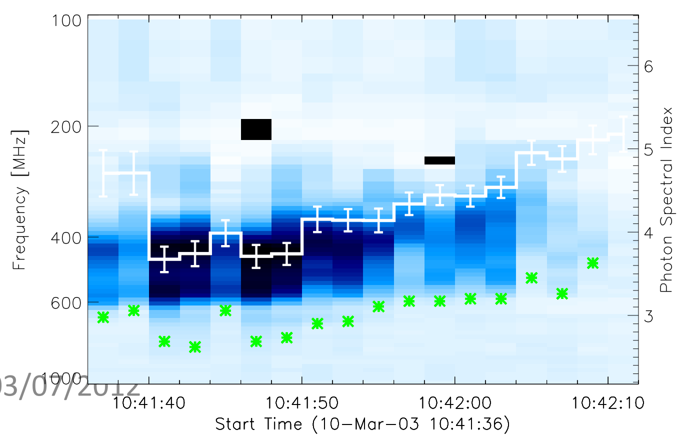
Frequency [MHz]
Photon Spectral Index
Start Time (10–Mar–03 10:41:36)

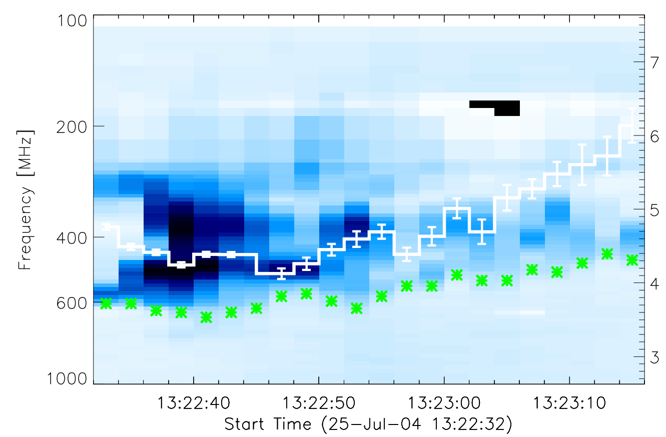
Frequency [MHz]
Photon Spectral Index
Start Time (25–Jul–04 13:22:32)

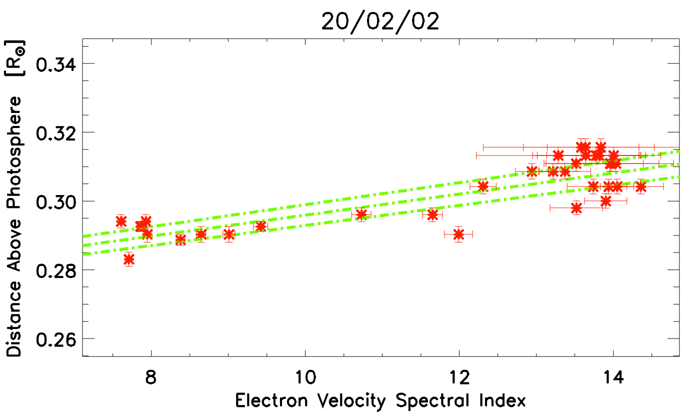
20/02/02
Distance Above Photosphere [R⊙]
0.34
0.32
0.30
0.28
0.26
8
10
12
14
Electron Velocity Spectral Index

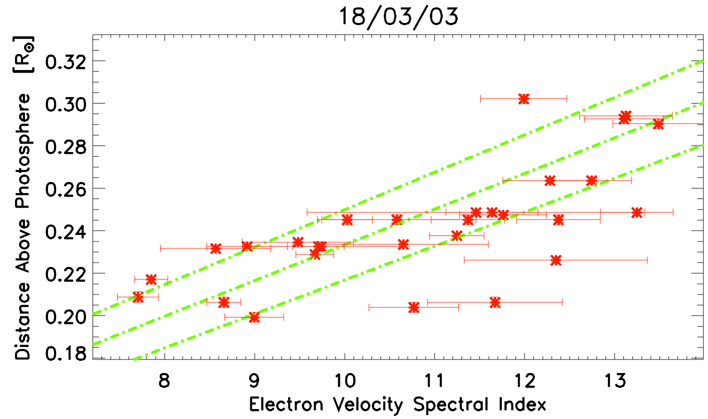
18/03/03
Distance Above Photosphere [R⊙]
0.32
0.30
0.28
0.26
0.24
0.22
0.20
0.18
8
9
10
11
12
13
Electron Velocity Spectral Index

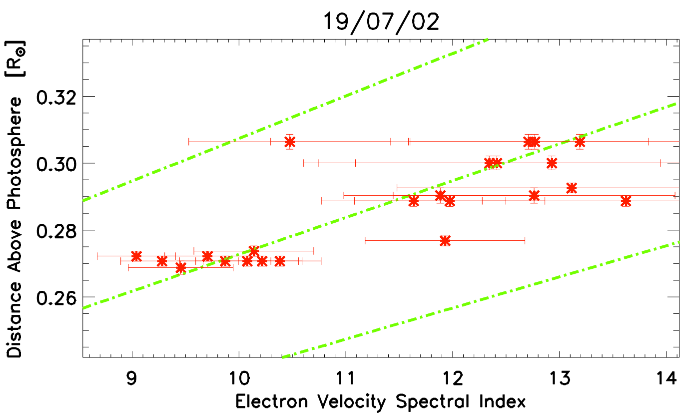
19/07/02
Distance Above Photosphere [R⊙]
0.32
0.30
0.28
0.26
9
10
11
12
13
14
Electron Velocity Spectral Index

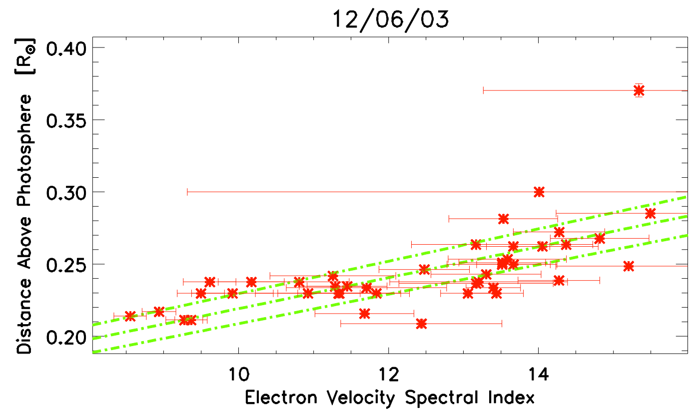
12/06/03
Distance Above Photosphere [R⊙]
0.40
0.35
0.30
0.25
0.20
10
12
14
Electron Velocity Spectral Index

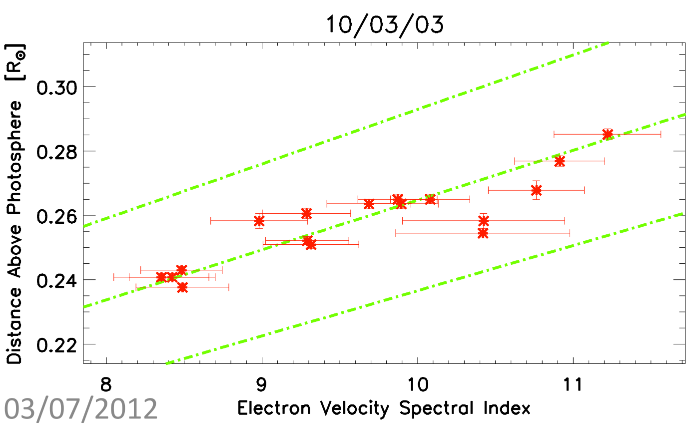
10/03/03
Distance Above Photosphere [R⊙]
0.30
0.28
0.26
0.24
0.22
8
9
10
11
Electron Velocity Spectral Index

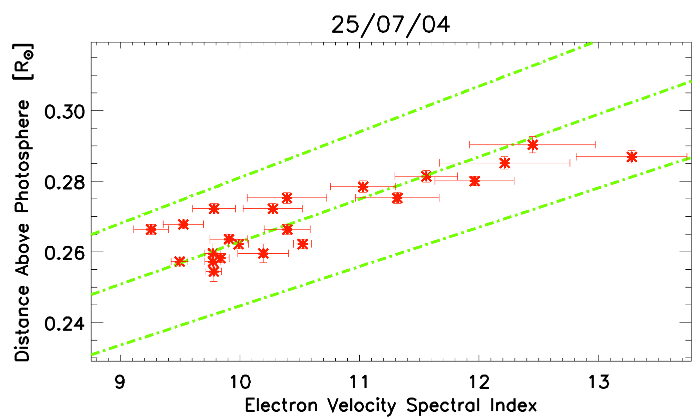
25/07/04
Distance Above Photosphere [R⊙]
0.30
0.28
0.26
0.24
9
10
11
12
13
Electron Velocity Spectral Index

Example of some Type III Solar Radio Bursts using WAVES

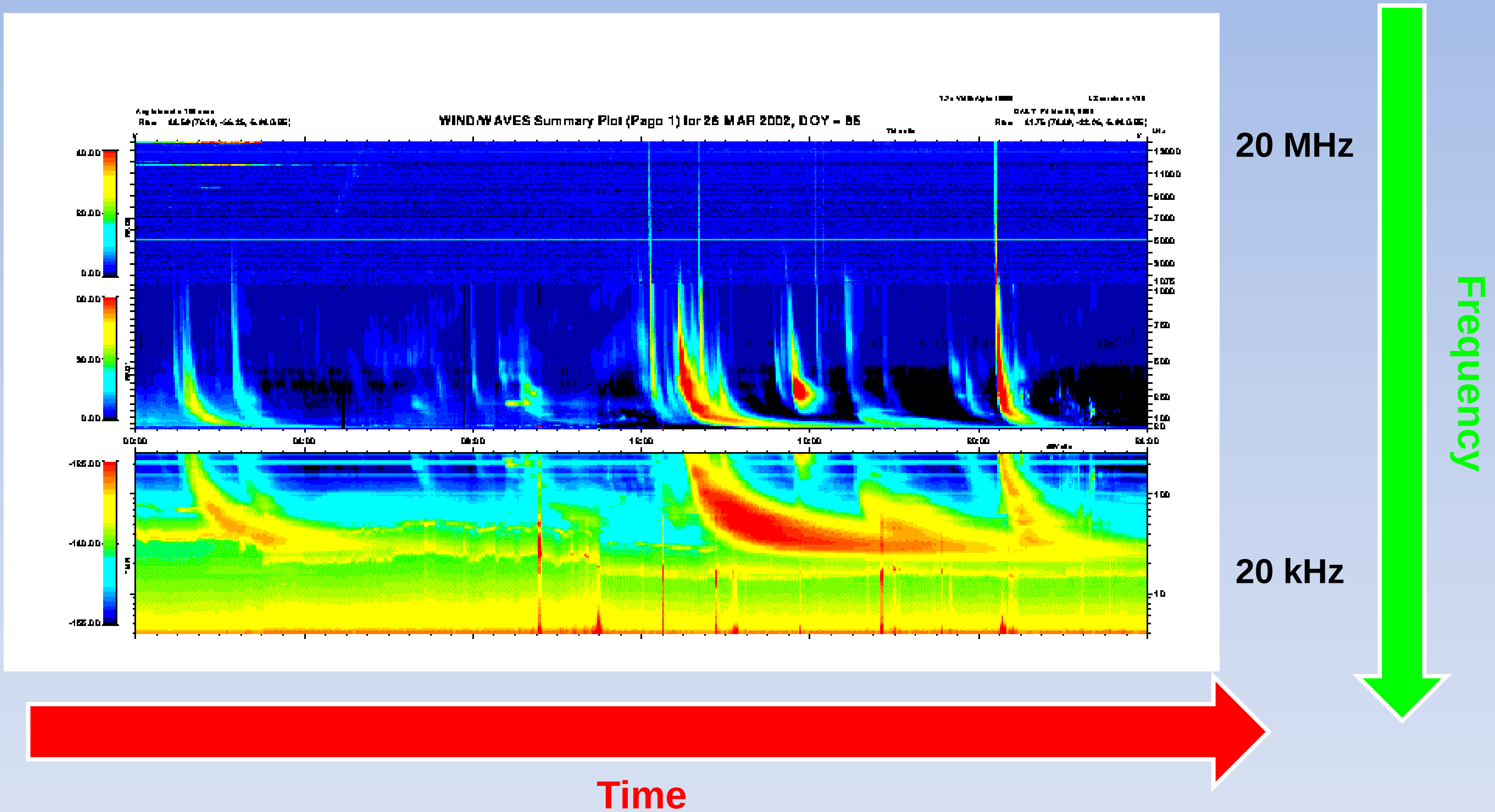

One Dimensional Quasilinear Equations

One dimensional quasilinear equations (e.g. Drummond and Pines, 1962) describing the kinetics of energetic electrons and Langmuir waves (Kontar, 2001) (Reid and Kontar 2010 in press ApJ)

$$\frac{\partial F}{\partial t} + \frac{v}{(r+r_0)^2}\frac{\partial}{\partial r}(r+r_0)^2 f = \frac{4\pi^2 e^2}{m^2}\frac{\partial}{\partial v}\left(\frac{W}{v}\frac{\partial F}{\partial v}\right) - \gamma_c \frac{d}{dv}\left(\frac{f}{v^2}\right)$$

$$\frac{\partial W}{\partial t} + \frac{v^2}{L}\frac{\partial W}{\partial v} + \frac{3v_{Te}^2}{v}\frac{\partial W}{\partial r} = \frac{\pi\omega_{pe}}{n_e} v^2 W \frac{\partial F}{\partial v} - (\gamma_{cw} + \gamma_L)W + \gamma_s v F \log\left(\frac{v}{v_t}\right)$$

Wave Generation and Absorption

Spontaneous Emission

$$\omega_{pe} = kv$$

One Dimensional QL equations

One dimensional quasilinear equations (e.g. Drummond and Pines 1962, Vedenov et al 1962) describing the resonant interaction between energetic electrons and Langmuir waves.

$$\frac{\partial F}{\partial t} = \frac{4\pi^2 e^2}{m^2}\frac{\partial}{\partial v}\left(\frac{W}{v}\frac{\partial F}{\partial v}\right)$$

$$f(v, t=0) = \frac{2n_b v}{v_0^2}$$

$$\frac{\partial W}{\partial t} = \frac{\pi\omega_{pe}}{n_e} v^2 W \frac{\partial F}{\partial v}$$

$$\omega_{pe} = kv$$

Quasilinear Relaxation

Electron Distribution

Langmuir Wave Distribution

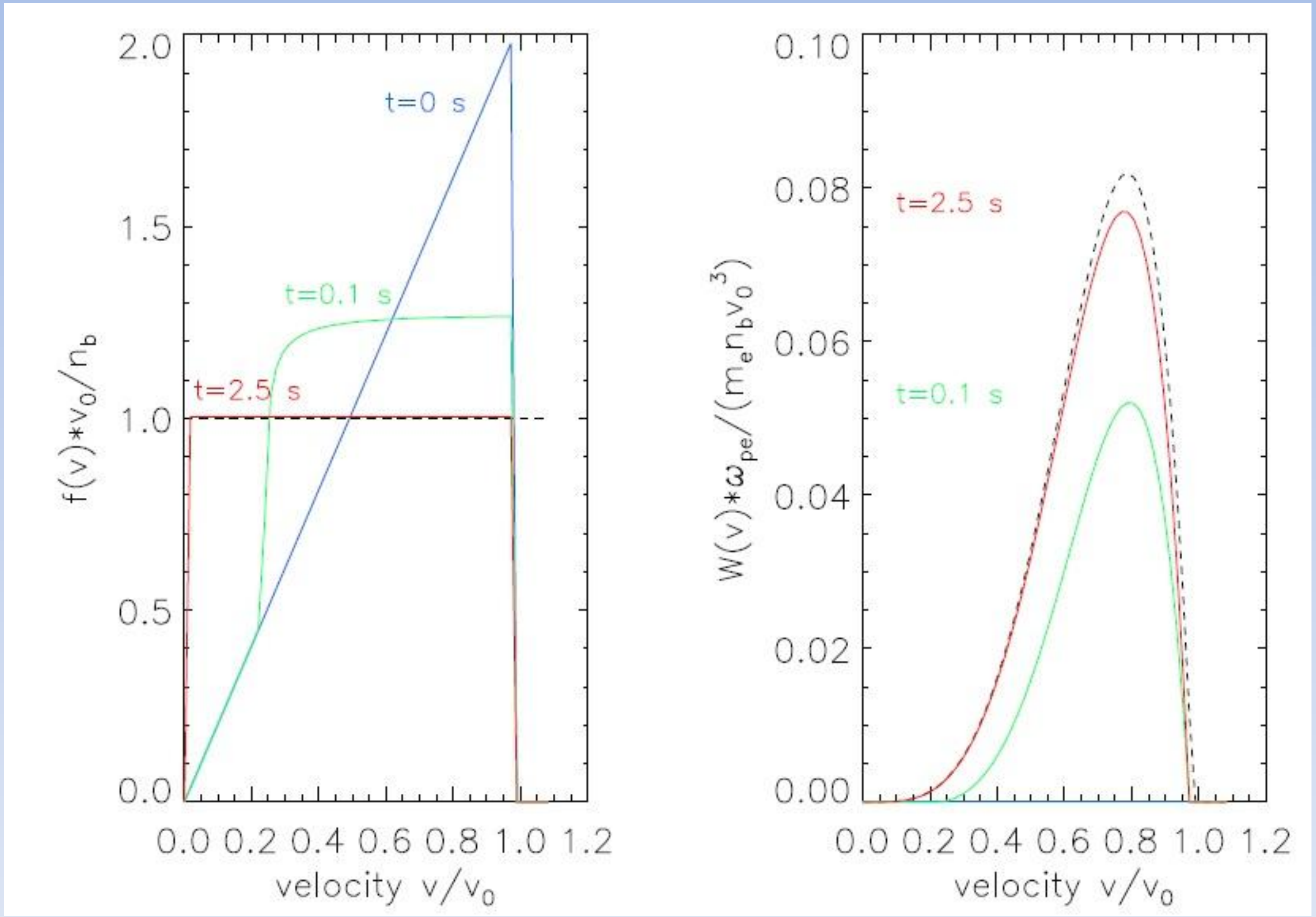

One Dimensional QL equations

One dimensional quasilinear equations (e.g. Drummond and Pines 1962, Vedenov et al 1962) describing the resonant interaction between energetic electrons and Langmuir waves. (e.g. Kontar 2001)

$$L = 2n_e\left(\frac{\partial n_e}{\partial x}\right)^{-1}$$

$$\frac{\partial F}{\partial t} = \frac{4\pi^2 e^2}{m^2}\frac{\partial}{\partial v}\left(\frac{W}{v}\frac{\partial F}{\partial v}\right)$$

$$f(v, t=0) = \frac{2n_b v}{v_0^2}$$

$$\frac{\partial W}{\partial t} + \frac{v^2}{L}\frac{\partial W}{\partial v} = \frac{\pi\omega_{pe}}{n_e}v^2 W\frac{\partial F}{\partial v}$$

$$\omega_{pe} = kv$$

Background Plasma Inhomogeneity

Quasilinear Relaxation and Density Inhomogeneity

Langmuir Wave Distribution

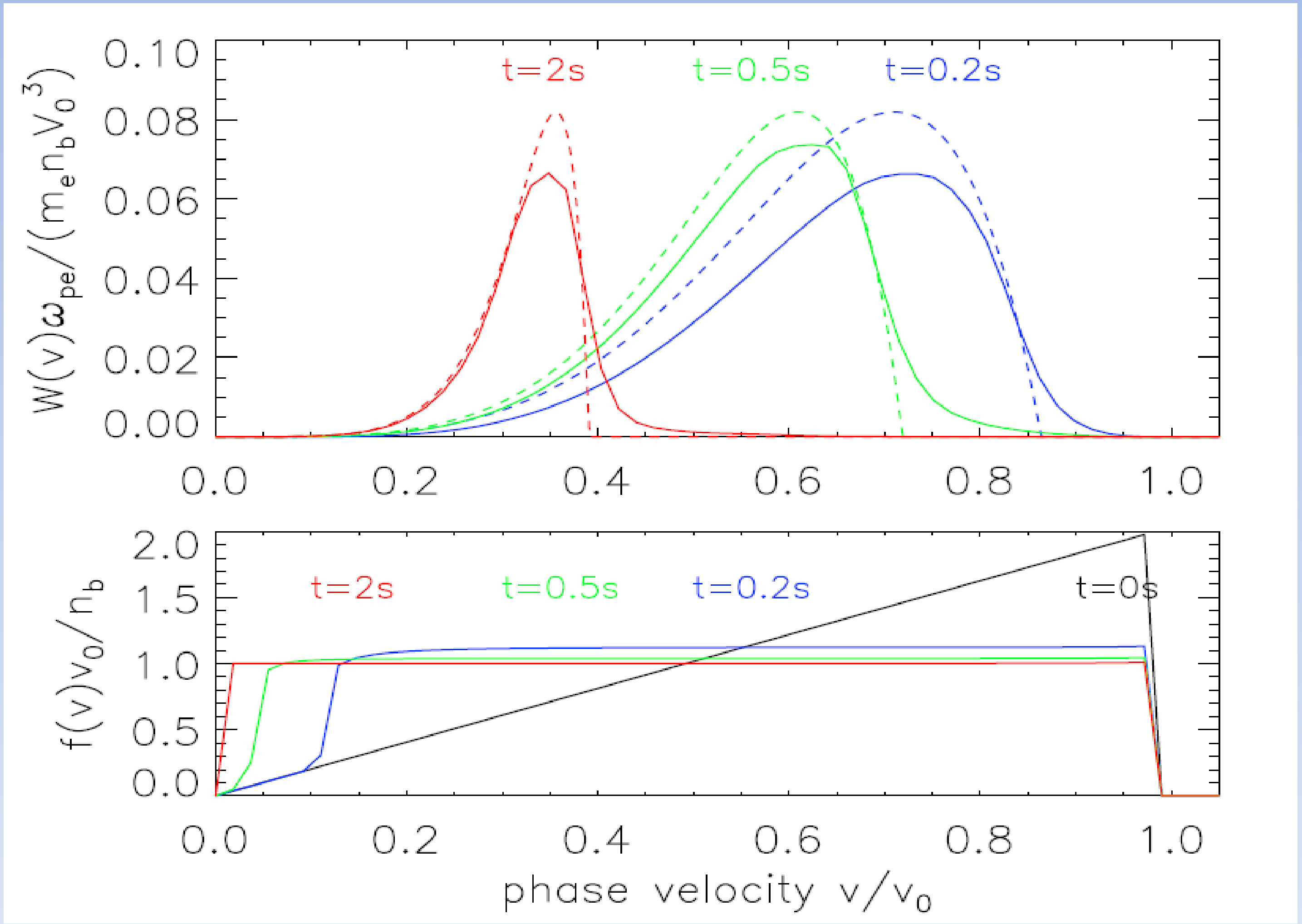

Electron Distribution

Time dependent injection

Consider an electron cloud with size **d**, spectral index α located at initial acceleration site r**=0** with characteristic injection time τ described by:

$$f_0(v,r,t=0) = g_0(v)\exp\left(\frac{-|r|}{d}\right)A(\tau)\exp\left(\frac{-|t-t_0|}{\tau}\right)$$

$$g_0(v) \sim v^{-\alpha}$$

Langmuir waves are generated when their growth rate is larger than the background Maxwellian plasma collisional absorption.

$$\gamma = \frac{\pi\omega_{pe}}{n}v^2\frac{\partial f}{\partial v} > \nu_c \qquad \nu_c = \frac{\omega_{pe}^2 e^2}{4m_e v_{Te}^3}\ln\Lambda$$

Time dependent injection

Using the same technique as previously and assuming the collisional absorption is small we get a relation which causes Langmuir waves generation to be dependent upon both the characteristic size and time

$$h_{typeIII} = (d + v\tau)\alpha + h_{acceleration}$$

Assuming a characteristic velocity of 10^{10} cm/s we find that time injection affects the starting frequency when it is greater than roughly 0.2 s.